EJNMMI Physics

ORIGINAL RESEARCH

Open Access

Feasibility of shortening scan duration of ^{18}F-FDG myocardial metabolism imaging using a total-body PET/CT scanner

Xiaochun Zhang[1†], Zeyin Xiang[1†], Fanghu Wang[1], Chunlei Han[2], Qing Zhang[1], Entao Liu[1], Hui Yuan[1*] and Lei Jiang[1,3*]

[†]Xiaochun Zhang and Zeyin Xiang contributed equally to this work.

*Correspondence:
Hui Yuan
oliver.yh@outlook.com;
yuanhui@gdph.org.cn
Lei Jiang
jianglei6814@gdph.org.cn;
leijiang1031@163.com
[1]PET Center, Department of Nuclear Medicine, Guangdong Provincial People's Hospital (Guangdong Academy of Medical Sciences), Southern Medical University, 106 Zhongshan Er Road, Guangzhou 510080, China
[2]Turku PET Centre, Turku University Hospital, Turku, Finland
[3]Guangdong Provincial Key Laboratory of Artificial Intelligence in Medical Image Analysis and Application, Guangzhou, China

Abstract

Purpose To evaluate ^{18}F-FDG myocardial metabolism imaging (MMI) using a total-body PET/CT scanner and explore the feasible scan duration to guide the clinical practice.

Methods A retrospective analysis was conducted on 41 patients who underwent myocardial perfusion-metabolism imaging to assess myocardial viability. The patients underwent ^{18}F-FDG MMI with a total-body PET/CT scanner using a list-mode for 600 s. PET data were trimmed and reconstructed to simulate images of 600-s, 300-s, 120-s, 60-s, and 30-s acquisition time (G600-G30). Images among different groups were subjectively evaluated using a 5-point Likert scale. Semi-quantitative evaluation was performed using standardized uptake value (SUV), myocardial to background activity ratio (M/B), signal to noise ratio (SNR), contrast to noise ratio (CNR), contrast ratio (CR), and coefficient of variation (CV). Myocardial viability analysis included indexes of Mismatch and Scar. G600 served as the reference.

Results Subjective visual evaluation indicated a decline in the scores of image quality with shortening scan duration. All the G600, G300, and G120 images were clinically acceptable (score ≥ 3), and their image quality scores were 4.9 ± 0.3, 4.8 ± 0.4, and 4.5 ± 0.8, respectively ($P > 0.05$). Moreover, as the scan duration reduced, the semi-quantitative parameters M/B, SNR, CNR, and CR decreased, while SUV and CV increased, and significant difference was observed in G300-G30 groups when comparing to G600 group ($P < 0.05$). For myocardial viability analysis of left ventricular and coronary segments, the Mismatch and Scar values of G300-G30 groups were almost identical to G600 group (ICC: 0.968-1.0, $P < 0.001$).

Conclusion Sufficient image quality for clinical diagnosis could be achieved at G120 for MMI using a total-body PET/CT scanner, while the image quality of G30 was acceptable for myocardial viability analysis.

Keywords Myocardial metabolism imaging (MMI), ^{18}F-FDG, Total-body PET/CT, Scan duration

Introduction

Myocardial metabolism imaging (MMI) together with myocardial perfusion imaging (MPI) are the gold standard technique for evaluating myocardial viability [1], which is critical for defining coronary artery revascularization to improve left ventricular (LV) function and reduce adverse cardiac events [2, 3]. Glucose is one of the sources of myocardial energy. ^{18}F-FDG MMI can reflect the ability of the myocardium to uptake and utilize glucose [4]. According to the American Society of Nuclear Cardiology (ASNC) imaging guidelines and the Society of Nuclear Medicine and Molecular Imaging (SNMMI) procedure standard, MMI acquisition is usually performed on the PET/CT scanner for 10–30 min [5]. However, the routine clinical applications of MMI often require consideration of scan duration and patient tolerance. Tolerance issue mainly occurs in some patients with severe heart failure, who may experience difficulty breathing due to prolonged supine position and are unable to complete the acquisition [6, 7]. It also exists in some infants and children for whom myocardial viability evaluation is needed due to cardiovascular malformations, often requiring sedation due to inability to actively complete the acquisition [8–10].

In recent years, the significant progress in the advancement of the availability of long-axial field of view (FOV) PET scanners and total-body PET scanners has substantially increased the sensitivity of PET/CT to detecting emitted photons and made it possible to acquire images with reduced time/dose but uncompromised image quality [11–13]. Nevertheless, as the evaluation of myocardial viability encompasses a spectrum of divergent imaging techniques in stages such as patient preparation, image acquisition, reconstruction, processing, and interpretation, it remains unclear whether these findings drawn from prior investigations utilizing a total-body PET/CT scanner are pertinent for MMI [5]. Therefore, this study aimed to investigate ^{18}F-FDG MMI using a total-body PET/CT scanner, and explore the feasible scan duration for clinical diagnosis and myocardial viability analysis.

Materials and methods

Patients

Between June 2023 and December 2023, the consecutive patients with confirmed or suspected coronary heart disease (CHD) who underwent MPI-MMI at our hospital to evaluate myocardial viability were retrospectively analyzed. The exclusion criteria were: (1) patients with severe arrhythmia; (2) patients with diabetes that leads to poor myocardial ^{18}F-FDG uptake; (3) patients with motion artifacts caused by physical movement during the acquisition. Finally, a total of 41 patients were enrolled. Patient characteristics were collected, including age, gender, body mass index (BMI), smoking history, hypertension, diabetes, hyperlipidemia, myocardial infarction and coronary revascularization history.

Image acquisition and reconstruction

Among 41 patients, 17 patients underwent ^{99m}Tc-MIBI SPECT MPI, while 24 patients underwent ^{13}N-NH_3 PET/CT MPI. SPECT MPI scans (Discovery 670, GE Healthcare, USA) were performed at 120 min after patients were intravenously injected with approximately 740 MBq (20 mCi) ^{99m}Tc-MIBI, and images were constructed by ordered subset expectation maximization (OSEM, 8 subsets, 4 iterations) algorithm. Besides, 10-min continuous PET/CT MPI scans (uEXPLORER, United Imaging Healthcare, Shanghai,

China) were performed in patients immediately after the bolus injection of approximately 370–555 MBq (10–15 mCi) ^{13}N-NH_3, and images were constructed using OSEM (20 subsets, 3 iterations, FWHM = 3.0 mm) algorithm.

For MMI, all patients fasted for at least 6 h, and the standard protocol of oral glucose load and insulin injection was applied based on diabetic status and blood glucose level. ^{18}F-FDG was intravenously injected at a dose of 3.7 MBq/kg (0.1 mCi/kg) after the blood glucose level was ≤7.8 mmol/L. Approximately 90 min after injection, the patients underwent MMI for 600 s on the total-body PET/CT scanner. PET images were reconstructed using the OSEM (20 subsets, 3 iterations, matrix: 192×192, pixel size: 2.34×2.34×2.89 mm^3, FWHM = 3.0 mm) algorithm and CT-based attenuation correction was applied. From the beginning of acquisition, all 600-s MMI list-model data were trimmed and reconstructed to simulate images of 600-s, 300-s, 120-s, 60-s, and 30-s acquisition time, which were defined as G600, G300, G120, G60, and G30, respectively. G600 served as the reference and was compared with other groups, with inter-frame co-registration performed.

Subjective visual evaluation

The image quality of MMI was subjectively and independently evaluated by two experienced nuclear medicine physicians (XC Zhang and H Yuan), each with a minimum of ten years of experience. A 5-point Likert scale was used for evaluating overall impression of the image quality, image noise, and conspicuity of lesions [14, 15]. Scores of 5 to 1 that were defined as follows: 5-excellent: conspicuity of lesions was clearly defined and noise was almost imperceptible; 4-good: conspicuity of lesions was fairly defined and noise was lower than the regular image of daily practice; 3-average: conspicuity of lesions and noise were equivalent to the regular image of daily practice obtained using conventional PET/CT scanner in our hospital; 2-poor: conspicuity of lesions was ill defined and noise was worse than the regular image of daily practice; and 1-very poor: conspicuity of lesions was un-recognizable and noise was excessive. Images with score 5 to 3 could meet the needs of clinical diagnosis. Specifically, image noise and lesion visibility were not further scored separately, as it simplifies the research process, makes the results more clinically applicable, reduces the collinearity, and exhibits high inter-observer consistency. Additionally, any disagreement between two physicians was resolved by consensus.

Semi-quantitative evaluation

The LV myocardium was automatically segmented using Carimas v 2.10 software (Turku PET Centre, Finland) to obtain volume of interest (VOI), and the VOI of LV blood pool was also semi-automatically delineated (manually adjusted to avoid the myocardial wall and papillary muscles) [16]. All VOIs were drawn on G600 images and applied to G300, G120, G60, and G30 images to ensure consistency in the location and size of VOIs among different groups (Fig. 1). The following standardized uptake values (SUVs) were measured using LIFEx software: SUV_{max}, SUV_{mean}, and SUV_{SD} of the LV myocardium (SUV_{max}MYO, SUV_{mean}MYO, and SUV_{SD}MYO), and SUV_{max}, SUV_{mean}, and SUV_{SD} of the LV blood pool (SUV_{max}LV, SUV_{mean}LV, and SUV_{SD}LV) [17]. Subsequently, the indexes of myocardial to background activity ratio (M/B), signal to noise ratio (SNR), contrast to noise ratio (CNR), contrast ratio (CR), and coefficient of variation (CV) were calculated as [18]: M/B = SUV_{max}MYO/SUV_{max}LV, SNR = SUV_{mean}MYO/

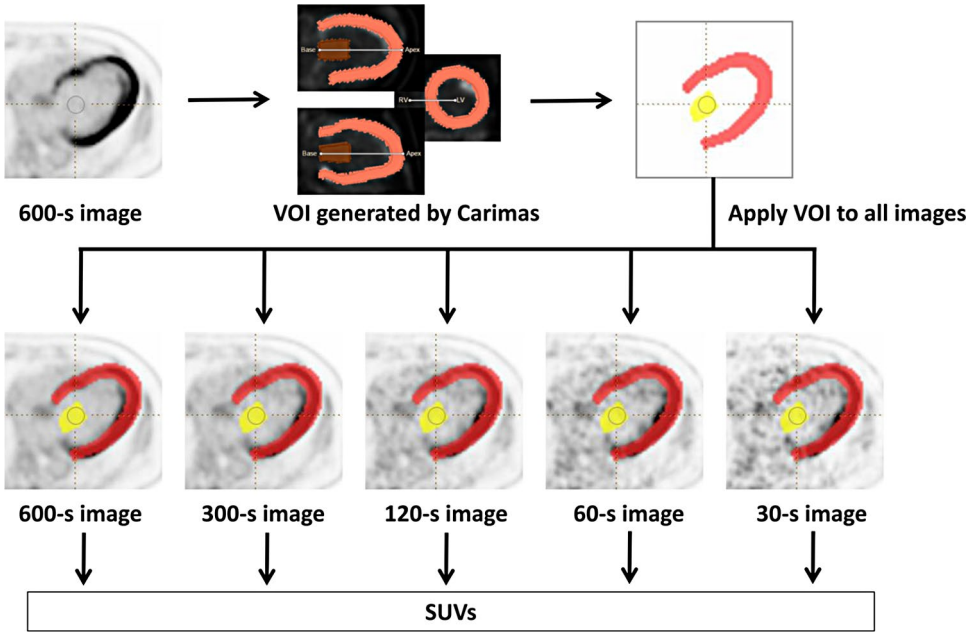

Fig. 1 Flowchart of segmentation of the left ventricular myocardium using Carimas software

$SUV_{SD}LV$, $CNR=(SUV_{mean}MYO-SUV_{mean}LV)/SUV_{SD}LV$, $CR=SUV_{mean}MYO/SUV_{mean}LV$, and $CV=SUV_{SD}MYO/SUV_{mean}MYO$.

Myocardial viability analysis

According to the American Heart Association (AHA) standards, the LV myocardium in MPI and MMI was displayed in polar maps and segmented into three coronary segments for analysis using the commercial specialized QGS+QPS software package (Cedars-Sinai Medical Center, USA). If the pixel value of the myocardial image was higher than 80% of the maximum perfusion or metabolism activity, it was defined as normal, otherwise, it was defined as abnormal [19]. Total perfusion defect (TPD) (%) was generated by the MPI polar map, representing the extent and severity of the hypoperfused myocardium. Then, pixel-by-pixel comparison was performed between the MPI polar map and the MMI polar map to generate polar maps of Mismatch and Scar. Mismatch (%) was the percentage of the LV myocardium with abnormal perfusion and normal metabolism, representing the amount of the mismatched (viable) myocardium. Scar (%) was the percentage of the LV myocardium both with abnormal perfusion and metabolism, representing the amount of the matched (scarred) myocardium.

Statistical analysis

Statistical analysis was performed using SPSS 26.0 software (IBM SPSS Inc, USA). Continuous variables were expressed as mean±standard deviation (SD) or median (range) upon the normality, while count variables were expressed in numbers or percentages. The agreement of image scores between two physicians was measured with the kappa test, and a kappa value≥0.81 was considered excellent agreement. The subjective image quality between acquisition time groups (G300-G30 vs. G600) was compared using Kruskal Wallis rank sum test and Dunn's post hoc test. The objective image quality between groups was compared using paired t-test or Wilcoxon test. Mismatch and Scar

indexes among groups were analyzed using intra class correlation coefficient (ICC) and Bland-Altman plot. All statistical tests were two-tailed, with $P<0.05$ indicating statistical significance.

Results

Patient characteristics

The enrolled 41 patients consisted of 36 males and 7 females, with an average age of 57.6 years (range, 35–75 years). The average BMI of these patients was 24.0±3.6 kg/m^2. Among 41 patients, 12 (29%), 20 (49%), 11 (27%), and 9 (22%) patients had the clinical history of smoking, hypertension, diabetes, and hyperlipidemia, respectively. Additionally, 27 out of 41 patients (66%) presented with the history of myocardial infarction, and 9 patients (22%) had undergone revascularization. The characteristics of these patients were summarized in Table 1.

Subjective visual evaluation

The agreement of image scores showed a kappa value of 0.887 between two physicians. The assessed results of subjective image quality using a 5-point Likert scale across different PET MMI scan duration were listed in Fig. 2. It indicated a decline in the scores of image quality with reduced scan duration. 87.8% of the G600 cases, 78.0% of the G300 cases, and 63.4% of the G120 cases were evaluated as the score of 5, and all the G600, G300, and G120 images were clinically acceptable (score≥3). The overall image quality scores of G600, G300, and G120 groups were 4.9±0.3, 4.8±0.4, and 4.5±0.8, respectively, and there was no significant difference among these scan duration groups ($P>0.05$). Additionally, there was a significant decrease in the scores of G60 (3.6±0.7) and G30 (2.5±0.8) groups when compared to G600 images ($P<0.05$).

Semi-quantitative evaluation

As shown in Table 2, there was a significant difference in the SUV_{max}MYO, SUV_{max}LV, and SUV_{mean}LV of G300-G30 groups when compared to G600 group ($P<0.05$). The SUV_{mean}MYO of G300 and G120 groups was similar to that of G600 group ($P>0.05$), but significant difference was observed in G60 and G30 when compared to G600 ($P<0.05$). Moreover, there was a decline in the semi-quantitative parameters of M/B, SNR, CNR and CR, and an increase in CV with reduced scan duration. There was no significant difference in M/B between G300 and G600 groups ($P>0.05$), while M/B of G120-G30 groups was lower than that of G600 group ($P<0.05$). Additionally, the significant

Table 1 Patient characteristics

Characteristics	Value
Age (years)	57.6 ± 10.1
Male (%)	36 (87%)
BMI (kg/m^2)	24.0 ± 3.6
Smoking (%)	12 (29%)
Hypertension (%)	20 (49%)
Diabetes (%)	11 (27%)
Hyperlipidemia (%)	9 (22%)
Previous history of myocardial infarction (%)	27 (66%)
Previous history of revascularization (%)	9 (22%)

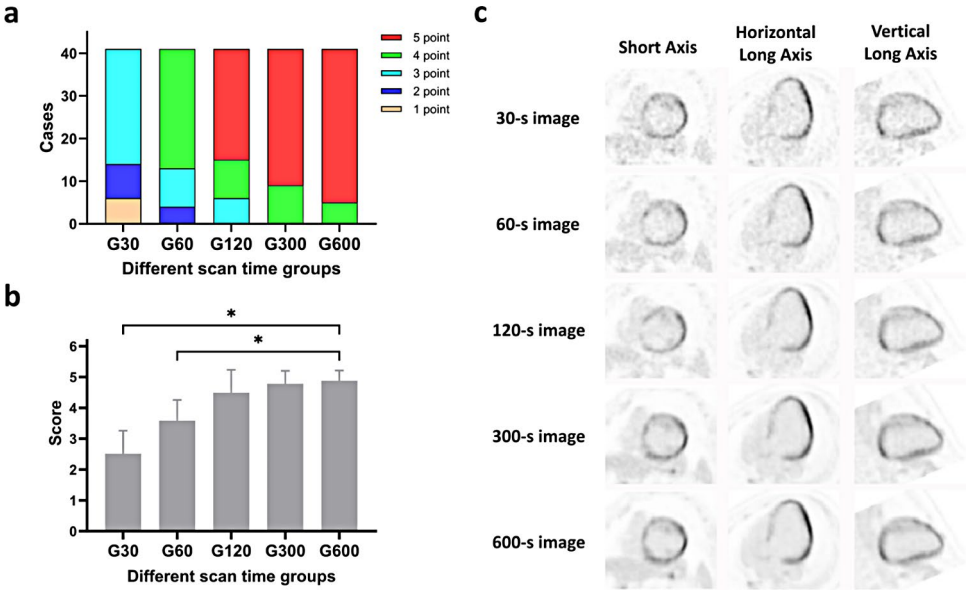

Fig. 2 Subjective visual evaluation with a 5-point Likert scale. a: Distribution of assessed scores among different scan duration groups. b: Comparison of visual evaluation scores among different scan duration groups (*$P<0.001$). c: ^{18}F-FDG MMI of different scan duration in a 51-year-old male patient with CHD. The image quality scores of the 600-s, 300-s, 120-s, 60-s, and 30-s scan duration were 5, 5, 5, 4, and 3 points, respectively

Table 2 Semi-quantitative evaluation of different scan duration groups

Scan duration	SUV_{max}MYO	SUV_{mean}-MYO	SUV_{max}LV	SUV_{mean}LV	M/B	SNR	CNR	CR	CV
G30	17.90 ± 5.89*	4.91 ± 2.12*	3.05 ± 1.10*	0.99 ± 0.33*	6.68 ± 3.50*	11.29 (6.91–15.98)*	8.53 (5.36–13.48)*	4.82 (3.31–7.31)*	0.52 (0.48–0.61)*
G60	16.14 ± 5.89*	4.95 ± 2.13*	2.18 ± 0.64*	0.97 ± 0.33*	8.11 ± 3.79*	16.78 (11.35–23.80)*	12.43 (8.06–20.41)*	4.81 (3.37–7.49)*	0.50 (0.43–0.57)*
G120	15.01 ± 5.81*	4.96 ± 2.14	1.79 ± 0.52*	0.96 ± 0.32*	9.18 ± 4.42*	23.79 (16.20-34.07)*	19.00 (12.17–29.46)*	5.07 (3.47–7.71)*	0.48 (0.42–0.54)*
G300	14.41 ± 5.70*	4.97 ± 2.15	1.47 ± 0.42*	0.94 ± 0.31*	10.54 ± 4.87	34.97 (25.50-50.34)*	24.74 (19.93–42.49)*	5.05 (3.53–7.77)*	0.48 (0.42–0.53)*
G600	13.99 ± 5.73	4.98 ± 2.17	1.37 ± 0.38	0.93 ± 0.31	10.79 ± 4.69	40.71 (34.11–65.58)	31.16 (25.94–56.81)	5.12 (3.53–7.92)	0.47 (0.41–0.53)

*Denotes significant difference when compared to G600 ($P<0.05$)

difference was observed in SNR, CNR, CR, and CV of G300-G30 groups when comparing to G600 group ($P<0.05$).

Myocardial viability analysis

The results of myocardial viability analysis were listed in Table 3. The Mismatch and Scar of the LV in G300-G30 groups were identical to G600 group ($P>0.05$). The analysis of ICC showed that the Mismatch and Scar of the LV in G300-G30 groups were also identical to G600 group (ICC: 1.00, $P<0.001$). Besides, the Mismatch and Scar of the coronary segments in G300-G30 groups were identical to G600 group ($P>0.05$), and ICC analysis of the Mismatch and Scar of the coronary segments in G300-G30 groups were also

Table 3 Myocardial viability indexes of the left ventricular and coronary segment among different scan duration groups

Scan duration	Left ventricular myocardium				Coronary segmental myocardium			
	Mismatch (%)	ICC	Scar (%)	ICC	Mismatch (%)	ICC	Scar (%)	ICC
G30	6.0 (12.0–25.0)	1.00	9.0 (2.5–15.0)	1.00	11.0 (3.0–23.0)	0.969	8.0 (2.0–21.0)	0.968
G60	6.0 (12.0–25.0)	1.00	9.0 (2.5–15.0)	1.00	11.0 (3.0–27.0)	0.988	8.0 (2.0–20.0)	0.989
G120	6.0 (12.0–25.0)	1.00	9.0 (2.5–15.0)	1.00	12.0 (3.0–28.0)	0.994	8.0 (2.0–21.0)	0.993
G300	6.0 (12.0–25.0)	1.00	9.0 (2.5–15.0)	1.00	13.0 (3.0–26.0)	0.993	8.0 (2.0–20.0)	0.994
G600	6.0 (12.0–25.0)	-	9.0 (2.5–15.0)	-	12.0 (3.0–26.0)	-	8.0 (1.0–20.0)	-

ICC denotes the intra class correlation coefficient between G600 and other groups

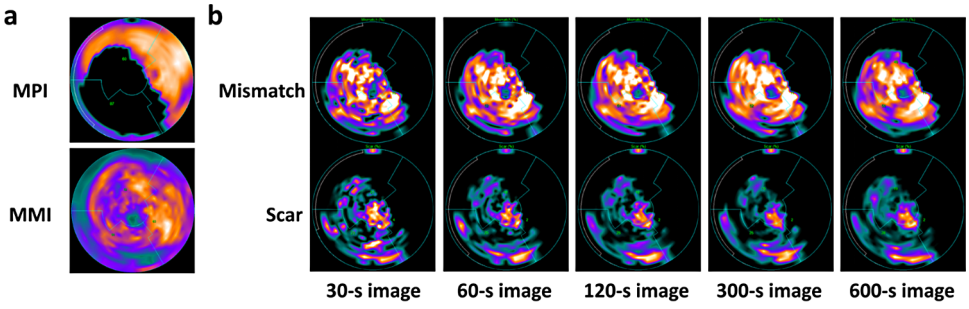

c

	Mismatch (%)					Scar (%)				
	G30	G60	G120	G300	G600	G30	G60	G120	G300	G600
LV	30	30	30	30	30	13	13	13	13	13
LAD	39	42	42	46	40	21	18	18	15	19
LCX	10	11	11	11	11	4	2	2	2	2
RCA	46	52	51	52	50	28	25	25	25	26

Fig. 3 Myocardial viability analysis in a 52-year-old male patient with CHD. **a**: Polar maps of myocardial perfusion imaging and myocardial metabolism imaging. **b**: Polar maps of Mismatch and Scar of different scan duration groups. **c**: Mismatch and Scar values for LV and coronary segments of different scan duration groups

identical to G600 group (ICC: 0.968–0.994, $P<0.001$) (Fig. 3). Similar results were also found in each of the three coronary segments (ICC: 0.920–0.998, $P<0.001$) (Table S1). Moreover, the Bland-Altman plots of the Mismatch and Scar of the coronary segments between G300-G30 and G600 groups were shown in Fig. 4.

Discussion

Myocardial viability analysis combining MPI and MMI is a critical procedure for patient stratification and treatment decisions, as revascularization treatment is more likely to salvage viable myocardium instead of scar [5]. Previous studies have found that the extent of viable myocardium in the infarct area was associated with treatment benefits [20, 21]. Hence, it is essential to evaluate the quality of myocardial images before the clinical diagnosis. Poor image quality such as image scores of 1–2 in subjective evaluations and M/B values lower than 2.2 in semi-quantitative evaluations might require repeated acquisition [22]. It is mainly due to that the radioactivity count of myocardium is low, while the background count is high; owing to the limitations of the reconstruction algorithm, Mismatch was often overestimated and Scar was underestimated [22]. As the novel hardware infrastructures and algorithm optimization allow the simultaneous recording of photons emitted from the whole body, compared to conventional PET/

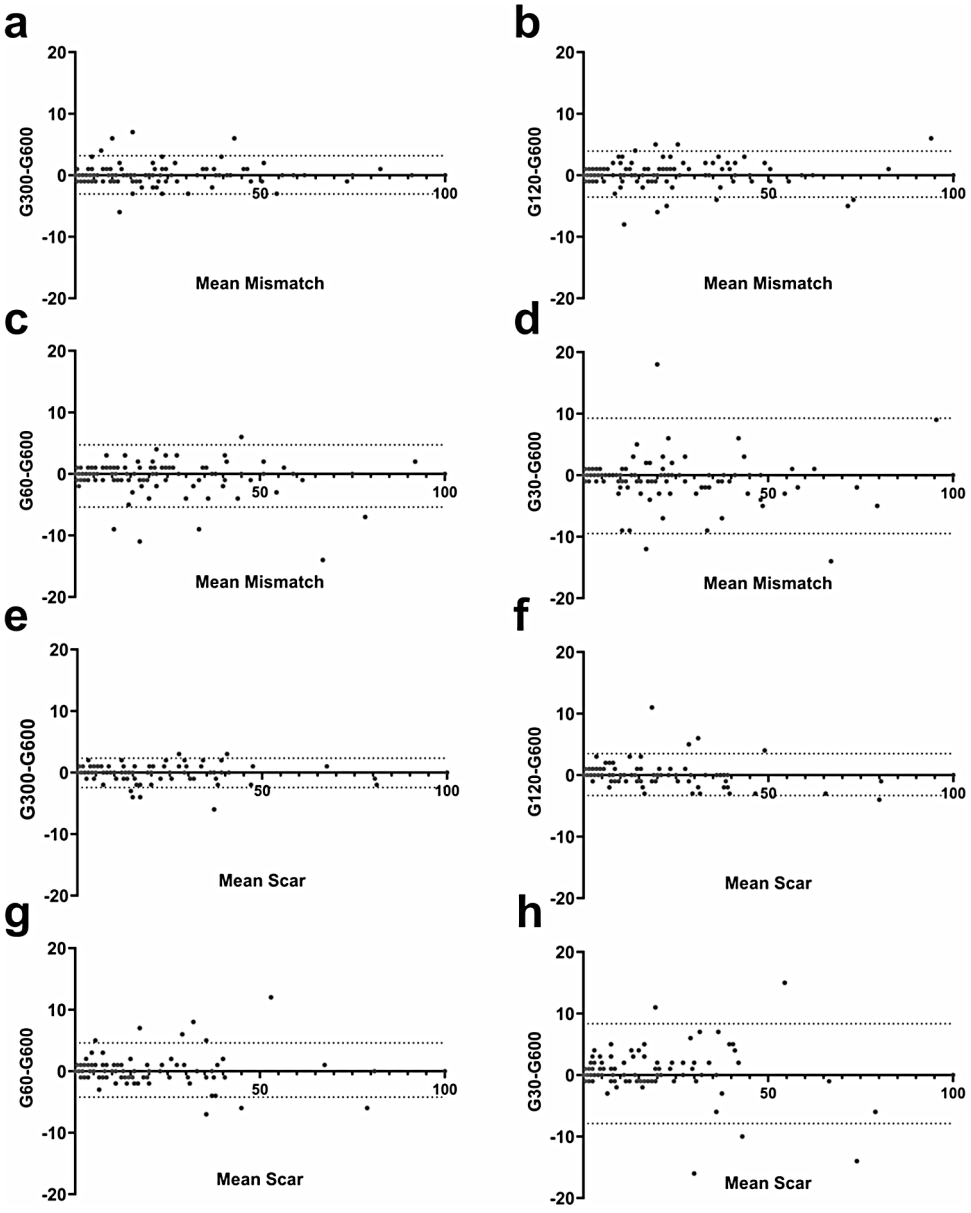

Fig. 4 Bland-Altman plot of Mismatch (**a**-**d**) and Scar (**e**-**h**) differences between G300-G30 and G600 in the coronary segment

CT scanners, total-body PET/CT scanners have significantly improved photon-detection rate by about 40 times, making it possible to acquire diagnostic value images with reduced scan duration or injected dose [11–13].

For subjective visual evaluation, the longer the scan duration performed, the better the image quality was. However, the current study showed that MMI PET images reached a similar quality at G120 (2 min) with G600 (10 min) using a total-body PET/CT scanner. This result was similar to the total-body PET/CT oncologic imaging study by Hu et al., who reported that the score of the 2-min image was roughly the same as 5-min image (4.80±0.42 vs. 5.00±0.00, $P>0.05$) [23]. Besides, in a head-to-head intra-individual comparison, Ian Alberts et al. found that long-axial PET/CT could deliver images of comparable subjective quality with a scan duration of less than 2 min compared to

conventional short-axial PET/CT acquired in 16 min [24]. Therefore, high quality images of MMI PET that met the clinical diagnostic requirements could be obtained at 2-min acquisition using a total-body PET/CT scanner, and subsequently, myocardial viability status in the hypo-perfused myocardium could be made by visual evaluation.

For semi-quantitative evaluation of MMI PET images, M/B is usually selected as the main indicator [22, 25]. M/B reflects the ratio of radiotracer distribution by myocardium and blood pool background. M/B difference of G600-G30 was analyzed in this study, which demonstrated that as the scan duration prolonged, M/B gradually increased. Although our study showed M/B at G120-G30 was significantly lower than G600, M/B at G60 (8.11 ± 3.79) using total-body PET/CT scanner was superior to the previous study at 10-min scan duration (6.87 ± 3.99) using conventional PET/CT scanner [22]. Besides, SNR is also an important index to characterize image quality. The higher SNR represents the less noise and the better image quality [26], which has been widely used in PET oncology imaging evaluation to investigate the feasibility of increasing lesion detection, reducing administrated dosage, and shortening scan duration [27–29]. Similar to the results of M/B, SNR results of G300-G30 were also lower when compared to G600. Schultz et al. investigated the impact of respiratory motion correction and attenuation correction on the image quality of MMI [18]. They employed different acquisition methods, and the median SNR value of the non-gated group with 24-min acquisition was 25.1 (range, 19.4–34.4), which was roughly consistent with the SNR value of 23.79 (range, 16.20-34.07) at 2-min acquisition of our study. Additionally, it is reported that CNR, CR, and CV can also be utilized for the semi-quantitative evaluation of MMI PET images [18]. Although this study demonstrated there were significant differences in these indexes at G300-G30 when compared to G600, they reached better levels at 1-min scan duration than other study at 24-min scan duration based on conventional PET/CT scanner.

Furthermore, the myocardial viability evaluation was analyzed on the basis of MMI PET images with shortening scan duration. Although there were some cases with the score of 1 or 2 images in G60 and G30 groups, surprisingly, the results of myocardial viability evaluation in G300-G30 groups were similar as G600. When the LV was used as the object of study, the Mismatch and Scar values of G300-G30 were identical to G600 with ICC of 1.0. When coronary segments were analyzed, the Mismatch and Scar of G300-G30 were almost identical to G600 with the ICC ranging from 0.968 to 0.994, which may be due to differences caused by manual segmentation, especially angle adjustment. During the routine clinical diagnosis, coronary segment analysis was more valuable than LV for selecting coronary arteries for revascularization [30].

Additionally, to reduce the computational and time cost for the imaging reconstruction, we adopted an axial FOV of 72 cm (3-bed units) covering from the upper chest to the upper abdomen, which we believe is a reasonable scan range to assure the integrity of the coverage of the heat, even in some case of inevitable position movement or severe cardiomegaly [31]. On the other hand, compared with conventional PET scanners, the extended axial FOV, novel crystal structures, and advanced imaging reconstruction algorithms have significantly enhanced performance in terms of energy resolution, time resolution, and counting rate, which may lead to better detection of myocardial metabolism activity. Although there have been no other studies to confirm this hypothesis in MMI studies, similar findings have been supported by other studies in oncological imaging.

For example, Zhao et al. found that pediatric patients undergoing total-body PET/CT showed no significant difference in lesion SUVmax and LBR down to 1/30 scan duration [15]. Tan et al. found no significant variance in average SUVmax and LBR of the lung, lymph nodes, and bone lesions between 2-min and 15-min images in a total-body PET/CT study of 28 lung cancer patients [11].

The clinical implications of reducing the scan duration of MMI are critically important. Firstly, it significantly enhances patient comfort during the examination, a factor that is especially crucial for patients suffering from heart failure. This adjustment also contributes to a substantial decrease in motion artifacts and hence, improved image quality. Secondly, it boosts the operational throughput and optimizes resource utilization and medical costs. Lastly, the strategy of minimizing the injection dose and concurrently extending the scan duration might contribute to the reduction of radiation exposure [23].

There are some limitations to this study. First, this was a single center, small sample study, and MPI consisted of SPECT and PET, all of which might lead to bias. Second, only the single-brand total-body PET/CT scanner was studied, which may warrant more exploration. Third, a head-to-head comparison of total-body PET/CT scanner in MMI with conventional PET/CT scanner was not performed. Fourth, myocardial viability imaging consisted of MPI and MMI, but this study only focused the feasibility of shortening scan duration of MMI, the exploration of the scan duration for MPI will be solved in the subsequent study.

Conclusion

Although the image quality of ^{18}F-FDG MMI with a total-body PET/CT scanner reduced with shortening scan duration, sufficient image quality for clinical diagnosis could be achieved at G120 for MMI using a total-body PET/CT scanner, while the image quality of G30 was acceptable for myocardial viability analysis.

Supplementary Information

The online version contains supplementary material available at https://doi.org/10.1186/s40658-024-00689-1.

Supplementary Material 1: Table S1. Myocardial viability indexes of each coronary segment among different scan duration groups.

Author contributions

Lei Jiang and Hui Yuan designed the study, Xiaochun Zhang, Zeyin Xiang and Fanghu Wang collected clinical and PET/CT data, Chunlei Han, Qing Zhang and Entao Liu helped with image processing, Xiaochun Zhang and Zeyin Xiang analyzed the data and carried out the statistical analysis. All authors wrote, read and approved the final manuscript.

Funding

This work was supported by Guangdong Province Medical Science and Technology Research Foundation (A2024039), National Natural Science Foundation of China (81971645), Guangdong Provincial People's Hospital (KY0120211130), and Guangdong Provincial Key Laboratory of Artificial Intelligence in Medical Image Analysis and Application (2022B1212010011).

Data availability

The datasets used and/or analyzed during the current study are available from the corresponding author on reasonable request.

Declarations

Ethics approval

The study was approved by the Ethics Committee of Guangdong Provincial People's Hospital and conducted following the principles of the 1964 Declaration of Helsinki and its later amendments or comparable ethical standards.

Consent to participate
Informed consent was waived due to the retrospective nature of this study.

Consent to publish
Yes.

Conflict of interest
The authors declare that they have no conflicts of interest.

Received: 12 May 2024 / Accepted: 3 October 2024
Published online: 11 October 2024

References

1. Tamaki N, Kawamoto M, Tadamura E, Magata Y, Yonekura Y, Nohara R, et al. Prediction of reversible ischemia after revascularization. Perfusion and metabolic studies with positron emission tomography. Circulation. 1995;91:1697–705.
2. Garcia MJ, Kwong RY, Scherrer-Crosbie M, Taub CC, Blankstein R, Lima J, et al. State of the art: imaging for myocardial viability: a Scientific Statement from the American Heart Association. Circ Cardiovasc Imaging. 2020;13:e000053.
3. Abraham A, Nichol G, Williams KA, Guo A, deKemp RA, Garrard L, et al. 18F-FDG PET imaging of myocardial viability in an experienced center with access to 18F-FDG and integration with clinical management teams: the Ottawa-FIVE substudy of the PARR 2 trial. J Nucl Med. 2010;51:567–74.
4. Peterzan MA, Lygate CA, Neubauer S, Rider OJ. Metabolic remodeling in hypertrophied and failing myocardium: a review. Am J Physiol Heart Circ Physiol. 2017;313:H597–616.
5. Dilsizian V, Bacharach SL, Beanlands RS, Bergmann SR, Delbeke D, Dorbala S, et al. ASNC imaging guidelines/SNMMI procedure standard for positron emission tomography (PET) nuclear cardiology procedures. J Nucl Cardiol. 2016;23:1187–226.
6. AbouEzzeddine OF, Lala A, Khazanie PP, Shah R, Ho JE, Chen HH, et al. Evaluation of a provocative dyspnea severity score in acute heart failure. Am Heart J. 2016;172:34–41.
7. Mebazaa A, Pang PS, Tavares M, Collins SP, Storrow AB, Laribi S, et al. The impact of early standard therapy on dyspnoea in patients with acute heart failure: the URGENT-dyspnoea study. Eur Heart J. 2010;31:832–41.
8. Yang M-F, Xie B-Q, Lv X-D, Hua Z-D, Duan F-J, Yan C-W, et al. The role of myocardial viability assessed by Perfusion/F-18 FDG Imaging in Children with Anomalous Origin of the left coronary artery from the pulmonary artery. Clin Nucl Med. 2012;37:44–8.
9. Zhang H-L, Li S-J, Wang X, Yan J, Hua Z-D. Preoperative evaluation and midterm outcomes after the Surgical correction of anomalous origin of the left coronary artery from the pulmonary artery in 50 infants and children. Chin Med J. 2017;130:2816–22.
10. Rickers C, Sasse K, Buchert R, Stern H, Van Den Hoff J, Lübeck M, et al. Myocardial viability assessed by positron emission tomography in infants and children after the arterial switch operation and suspected infarction. J Am Coll Cardiol. 2000;36:1676–83.
11. Tan H, Sui X, Yin H, Yu H, Gu Y, Chen S, et al. Total-body PET/CT using half-dose FDG and compared with conventional PET/CT using full-dose FDG in lung cancer. Eur J Nucl Med Mol Imaging. 2021;48:1966–75.
12. Cherry SR, Jones T, Karp JS, Qi J, Moses WW, Badawi RD, Total-Body PET. Maximizing sensitivity to Create New Opportunities for Clinical Research and Patient Care. J Nucl Med. 2018;59:3–12.
13. Badawi RD, Shi H, Hu P, Chen S, Xu T, Price PM, et al. First Human Imaging Studies with the EXPLORER Total-Body PET Scanner*. J Nucl Med. 2019;60:299–303.
14. Van Sluis J, Boellaard R, Somasundaram A, Van Snick PH, Borra RJH, Dierckx RAJO, et al. Image quality and semiquantitative measurements on the Biograph Vision PET/CT system: initial experiences and comparison with the Biograph mCT. J Nucl Med. 2020;61:129–35.
15. Zhao Y-M, Li Y-H, Chen T, Zhang W-G, Wang L-H, Feng J, et al. Image quality and lesion detectability in low-dose pediatric 18F-FDG scans using total-body PET/CT. Eur J Nucl Med Mol Imaging. 2021;48:3378–85.
16. Nesterov SV, Han C, Mäki M, Kajander S, Naum AG, Helenius H, et al. Myocardial perfusion quantitation with 15O-labelled water PET: high reproducibility of the new cardiac analysis software (Carimas™). Eur J Nucl Med Mol Imaging. 2009;36:1594–602.
17. Nioche C, Orlhac F, Boughdad S, Reuzé S, Goya-Outi J, Robert C, et al. LIFEx: a freeware for Radiomic feature calculation in Multimodality Imaging to accelerate advances in the characterization of Tumor Heterogeneity. Cancer Res. 2018;78:4786–9.
18. Schultz J, Siekkinen R, Tadi MJ, Teräs M, Klén R, Lehtonen E, et al. Effect of respiratory motion correction and CT-based attenuation correction on dual-gated cardiac PET image quality and quantification. J Nuclear Cardiol. 2022;29:2423–33.
19. Beanlands RSB, Ruddy TD, deKemp RA, Iwanochko RM, Coates G, Freeman M, et al. Positron emission tomography and recovery following revascularization (PARR-1): the importance of scar and the development of a prediction rule for the degree of recovery of left ventricular function. J Am Coll Cardiol. 2002;40:1735–43.
20. Ghosh N, Rimoldi OE, Beanlands RSB, Camici PG. Assessment of myocardial ischaemia and viability: role of positron emission tomography. Eur Heart J. 2010;31:2984–95.
21. Kandolin RM, Wiefels CC, Mesquita CT, Chong A-Y, Boland P, Glineur D, et al. The current role of viability imaging to Guide Revascularization and Therapy decisions in patients with heart failure and reduced left ventricular function. Can J Cardiol. 2019;35:1015–29.
22. Kobylecka M, Mazurek T, Fronczewska-Wieniawska K, Fojt A, Słowikowska A, Mączewska J, et al. Assessment of the myocardial FDG-PET image quality with the use of maximal standardized uptake value myocardial to background index. Application of the results in regard to semiquantitative assessment of myocardial viability with cardiac dedicated softwar. Nucl Med Rev. 2017;20:69–75.
23. Hu H, Huang Y, Sun H, Zhou K, Jiang L, Zhong J, et al. A proper protocol for routine 18F-FDG uEXPLORER total-body PET/CT scans. EJNMMI Phys. 2023;10:51.

24. Alberts I, Hünermund J-N, Prenosil G, Mingels C, Bohn KP, Viscione M, et al. Clinical performance of long axial field of view PET/CT: a head-to-head intra-individual comparison of the Biograph Vision quadra with the Biograph Vision PET/CT. Eur J Nucl Med Mol Imaging. 2021;48:2395–404.
25. Bax JJ, Veening MA, Visser FC, Van Lingen A, Heine RJ, Cornel JH, et al. Optimal metabolic conditions during fluorine-18 fluorodeoxyglucose imaging; a comparative study using different protocols. Eur J Nucl Med. 1997;24:35–41.
26. Buvat I, Castiglioni I. Monte Carlo simulations in SPET and PET. Q J Nucl Med. 2002;46:48–61.
27. Kadrmas DJ, Casey ME, Conti M, Jakoby BW, Lois C, Townsend DW. Impact of Time-of-flight on PET tumor detection. J Nucl Med. 2009;50:1315–23.
28. Kadrmas DJ, Oktay MB, Casey ME, Hamill JJ. Effect of scan time on oncologic lesion detection in whole-body PET. IEEE Trans Nucl Sci. 2012;59:1940–7.
29. Armstrong IS, Tonge CM, Arumugam P. Assessing time-of-flight signal-to-noise ratio gains within the myocardium and subsequent reductions in administered activity in cardiac PET studies. J Nuclear Cardiol. 2019;26:405–12.
30. Abazid RM, Romsa JG, Warrington JC, Akincioglu C, Smettei OA, Bureau Y, et al. Prognostic value of coronary computed tomography angiography compared to radionuclide myocardial perfusion imaging in patients with coronary stents. Front Cardiovasc Med. 2023;10:1087113.
31. Spencer BA, Berg E, Schmall JP, Omidvari N, Leung EK, Abdelhafez YG, et al. Performance evaluation of the uEXPLORER Total-Body PET/CT scanner based on NEMA NU 2-2018 with additional tests to characterize PET scanners with a long Axial Field of View. J Nucl Med. 2021;62:861–70.

Publisher's note